

# autoSFR: New Extensions to Automated Scanning Resolution Determination for Photographic Collections

Lei He, Phil Michel, Steven Puglia; Library of Congress; Washington, DC /USA; Don Williams; Image Science Associates; NY/USA

## Abstract

In this paper we present our recent software development, *autoSFR*, with new extensions to the previous program for automated scanning resolution determination, which was published in the paper “Computer Assisted Image Analysis for Objective Determination of Scanning Resolution for Photographic Collections – An Automated Approach” presented at Archiving 2013. The extension works include the algorithm robustness and accuracy verification by statistical tests, the analysis of denoising effects on the sampling efficiency computation, and the construction of a user friendly interface.

## 1. Introduction

Imaging quality analysis is crucial in digital preservation for archiving applications. A variety of standards have been established to assess different quality factors of imaging products, including resolution [1, 2, 3], intensity (e.g., OECF) [4] and color [5, 6] accuracy, noise [7], dynamic range [8], sharpness [1, 9], and geometric distortion [10], just to name a few. In this paper we focus on image sharpness assessment, which is probably the most important quality factor due to its role in determining the amount of detail that an imaging system can reproduce<sup>1</sup>. Furthermore, image sharpness is an indicator of imaging resolution.

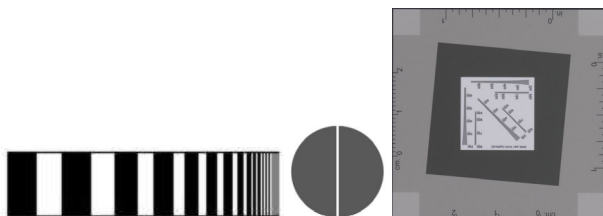


Figure 1. Examples of targets for MTF/SFR analysis. From left to right: sinusoidal, slit and slanted edge targets.

Image sharpness can be measured with subjective [11] and objective metrics [12, 13, 14], among which the *modulation transfer function* (MTF) [12, 13] or *spatial frequency response* (SFR) [14] are the most commonly used. MTF is defined as the modulation ratio of the output image and the ideal image, and SFR is a measurement of the effective system MTF relative to the test object feature used. Traditionally there are two types of methods to measure the MTF/SFR: direct methods evaluate the system response to periodic patterns (e.g., sine pattern bars); indirect

methods measure the *edge spread function* (ESF) of the system using slanted edges, or the *line spread function* (LSF) using slit targets, on which a frequency transform (e.g., Fourier transform) is then applied to derive the system frequency response. Figure 1 shows examples of the above three targets (test charts). Practically, indirect methods are always used due to their simple implementation. An excellent review on those approaches may be seen in [12].

The derived MTF/SFR provides a comprehensive overview of the imaging system performance across the whole frequency spectrum. Figure 2 compares two SFR curves. It can be seen that the system with red curve outperforms the one represented by the blue curve on both low and middle frequency signal reproduction. The interested reader is referred to the Federal Agencies Digitization Guidelines Initiative (FADGI)<sup>2</sup> for the details of SFR curve analysis. For a more direct assessment of imaging sharpness or comparison among different systems/images, we may compute the summary statistics from a SFR curve, e.g., sampling efficiency [15], which is currently embedded in the commercial software DICE<sup>TM</sup>. Given an input image, users are required to manually select the regions of interest (ROI) in DICE<sup>TM</sup>, i.e., regions with clear edges and low noise, for the SFR and sampling efficiency computation, which can then be used in the digitization production to determine an appropriate scanning resolution to capture information content. However, this process works well only for certain specifically designed target images which consist of small amount of edge regions, e.g., the GoldenThread Target<sup>3</sup>. It is infeasible to manually identify all the suitable ROIs in large collections of photographic images, due to the high labor cost, and the large intra- and inter-observer variations. In order to overcome these problems, we developed an automated image analysis approach [16] to derive an appropriate spatial or scanning resolution from image statistics. With predefined constraints on edges (e.g., contrast, orientation, and homogeneity) and SFR (e.g., curve shape and magnitude), our method identifies all the valid image edges, computes the SFR and sampling efficiency for each edge, and finally derives the optimal scanning resolution. In this paper we present our recent work to extend and upgrade this program: conducting statistical tests to verify the algorithm robustness and accuracy, analyzing the denoising effects on the SFR and sampling efficiency accuracy, and constructing a user friendly interface for the newer version software, *autoSFR*.

<sup>1</sup> Imatest – Sharpness: What is it and how is it measured?  
<http://www.imatest.com/docs/sharpness/>

<sup>2</sup> Guidelines – Federal Agencies Digitization Guidelines Initiative.  
<http://www.digitizationguidelines.gov/guidelines/>

<sup>3</sup> Image Science Associates. <http://www.imagescienceassociates.com/>

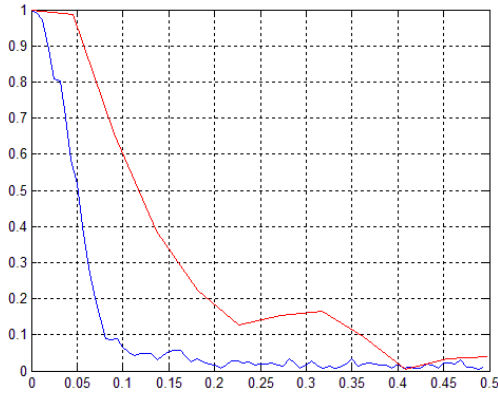


Figure 2. Examples of SFR curves derived from slanted edges.

This paper is organized as follows: Section 2 briefly introduces image quality and sharpness assessment technologies. Section 3 presents our extension works to the program and the new updated software, autoSFR. Experiment results on a large set of samples are presented in Section 4. We draw conclusions in Section 5.

## 2. Background

As introduced in Section 1, image quality assessment includes a variety of factors, such as sharpness, noise, dynamic range, color accuracy, and geometric distortion, which are defined by a series of corresponding international standards. In this work we focus on image sharpness analysis. There are usually three major sharpening processes<sup>4</sup> in a typical imaging pipeline: capture sharpening (through camera setting adjustment) for high resolution, image sharpening for better acutance [17], and output sharpening for print or display purposes. Image sharpening is usually implemented through image edge enhancement, such as filtering techniques using unsharp masks and inverse image diffusion. Output sharpening constructs profiles for individual output devices (printer or monitor) for the optimum print or display. With the objective to evaluate the imaging quality, we analyze image sharpness produced by the first type of sharpening, which is uniquely determined by the imaging systems.

Following the works in [12, 13, 14], we employ the commonly used MTF/SFR model to assess the image sharpness. Given square wave grating of different frequencies  $f$  (measured by the number of lines/mm), modulation is defined as

$$\text{Modulation} = (I_{\max} - I_{\min}) / (I_{\max} + I_{\min}) \quad (1)$$

where  $I_{\max}$  and  $I_{\min}$  are the maximum and minimum intensity measured in the image. The MTF is then defined as a function of the frequency, which is the modulation ratio of the output image and the input (ideal) image at different frequency measurements. Thus the value range of SFR is from 0 to 1, and the value monotonically decreases as the frequency increases. In practice,

scanners and cameras always apply certain image enhancement algorithms that are embedded into the imaging system to improve the sharpness quality in the output images, i.e., better acutance. This artificial sharpening also increases system responses (MTF values) at certain frequencies. For the objective of imaging quality assessment, such sharpening should always be avoided to maximally reflect the system true characteristics (i.e., optic and electronic hardware performance) in detail reproduction. In addition, such “soft” sharpening may cause over-sharpened images, with irritating halos at image edges.

Imaging quality assessment is usually implemented with specifically developed targets that consist of particular patterns, for example, the Gretag-Macbeth ColorChecker<sup>®</sup> SG for color accuracy assessment, a series of gray scale step wedges with increased density for OECF derivation and noise estimation, a Siemens Sinusoidal or Bitonal pattern for MTF/SFR computation [18], dead leaves pattern for texture SFR analysis [19], etc. In our digital preservation and conversion production, we utilize the GoldenThread Target to conduct a comprehensive imaging quality analysis in DICE<sup>™</sup>. This follows the procedures listed in the ISO 12233 [1] to compute the SFR: 1) locate the slanted edge regions; 2) compute the corresponding ESF (the profile across the edges) and LSF (the derivative of the ESF); and 3) calculate the Fourier transform of the LSF to derive the SFR. Slanted edges are used here to produce more samples on the ESF profile for more accurate LSF computation. This is implemented by projecting all points on multiple lines crossing the edge to one line, which produces sub-pixel resolution on the profile. Using such oversampled ESF, we can obtain more accurate results on the LSF and thus the SFR values. As indicated in the Introduction, such manual analysis cannot handle a large number of samples to determine scanning resolution. In particular, the labor and time cost will be significantly increased for challenging conditions like weak edges and noisy and inhomogeneous edge regions. Our early work [16] was proposed to overcome these problems for consistent results. In this paper, we further validate the accuracy and robustness of the algorithm.

The traditional MTF and SFR measurements provide a relatively simple model to conduct objective assessment of image sharpness. On the other hand, subjective measurements have been developed to address the factor of human visual perception (e.g., human eye’s contrast sensitivity function), such as the subjective quality factor [11] and acutance [17]. Moreover, with recent research on human visual system (HVS), more advanced models [20, 21] have been proposed to simulate human visual function. The interested reader is referred to [20] for an overview of no-reference image sharpness metrics.

## 3. Extended Work

This section presents the recent extension to our previously developed program [16] for automatic determination of the level of information content for photographic collections, and a corresponding spatial resolution for digitization. The algorithm description can be seen in Figure 2 of [16], which consists of main functions of valid edge detection, SFR and sampling efficiency computation, and scanning resolution determination. Our extended works include:

- Conducting statistical hypothesis tests to verify the robustness and accuracy of the program. We compare

<sup>4</sup> Cambridge in Colour – Photography Tutorials & Learning Community. <http://www.cambridgeincolour.com/>

the results from manual identification of edge regions by a content expert (the second author) and the automatic identification of edge regions by the program. With statistically similar results, we draw the conclusion that our program produces results comparable to the expert.

- Analyzing the denoising effects on SFR and sampling efficiency computation. For real sample collections, we always observe that the edge regions are noisy. We conduct this exploration with different denoising settings and determine that denoising has no significant effects on the SFR and sampling efficiency computation.
- Developing a user friendly interface for software distribution among different organizations.

In the extended work, we follow the algorithm flowchart in [16]. The program detects valid edges in each block of an input image sequentially, from which the corresponding SFR and sampling efficiency values are computed. Again, we apply the same edge, region, and SFR curve constraints on intensity and contrast to identify the valid edges.

The first experiment applies the two-sample  $t$ -test and  $F$ -test to check if two independent samples come from normal distributions with the same mean and variance, against the alternative that the means and variances are unequal [22]. Here the two samples are the sampling efficiencies computed from the valid edges identified by our expert and the program, respectively. Therefore, for the two-sample  $t$ -test, we have

$$H_0: \mu_e = \mu_p; \quad H_a: \mu_e \neq \mu_p. \quad (2)$$

where  $\mu_e$  represents the sampling efficiency mean obtained from the expert samples, and  $\mu_p$  represents the sampling efficiency mean from the samples produced by the program. Given the two sets of samples with the sample numbers  $n_e$  and  $n_p$ , we compute the statistics, i.e., sample mean  $\bar{\mu}_e$ ,  $\bar{\mu}_p$  and sample variance  $s_e^2$ ,  $s_p^2$ . We can obtain the following statistic

$$\frac{(\bar{\mu}_e - \bar{\mu}_p) - (\mu_e - \mu_p)}{\sqrt{\frac{s_e^2}{n_e^2} + \frac{s_p^2}{n_p^2}}} \quad (3)$$

that has a  $t$ -distribution with the number of degree of freedom as:

$$\frac{\left(\frac{s_e^2}{n_e^2} + \frac{s_p^2}{n_p^2}\right)^2}{\frac{s_e^2/n_e^2}{n_e-1} + \frac{s_p^2/n_p^2}{n_p-1}} \quad (4)$$

Then we can compute the  $p$ -value as the probability to obtain the statistics in Eqs. (3) and (4) under the assumption that the  $H_0$  is true, i.e.,  $\mu_e = \mu_p$ . In our experiments, we use Matlab<sup>TM</sup> Statistics Toolbox to compute this  $p$ -value. Similarly, we apply the same principle to conduct the two-sample  $F$ -test to compare the variances of the two samples.

Our second experiment analyzes the denoising effects on the SFR and sampling efficiency computation. With the observation

that real images are always contaminated by noise, our purpose here is to verify if the denoising operation helps improve the SFR and sampling efficiency. We use both synthetic and real samples in this experiment, and apply Gaussian noise to the synthetic edge image as a simple simulation to real cases. Gaussian filtering is used for denoising on the synthetic and real samples, i.e., the synthetic edge image with added noise and the detected edge regions in real samples. In the denoising filtering, we leave the narrow band surrounding the edge untouched in order to preserve the original edge features, i.e., we only smooth the regions far away from the edge. Thus there are two main parameters in the experiment, the denoising degree (strength) and the band size.

The third extension is to upgrade the user interface. Specifically, we construct the interface to allow for user input of the constraint parameters. The left figure of Figure 3 shows the interface with 14 textboxes for the constraint settings. These parameters are divided to two major categories for the edge detection and SFR computation constraints, respectively. Once a user clicks the “Go!” button, a dialog box pops up for the user to localize the configuration file that indicates the path and names of the samples. After the complete analysis on the samples, the final results are shown at the bottom of the interface window. In particular, the “Scanning Resolution” refers to the imaging setting when the samples were scanned (as reported in the file header); the “Efficiency” is derived by the center limit theorem (see [16] for details); the “Content Resolution” indicates the true level of information content for the sample set.

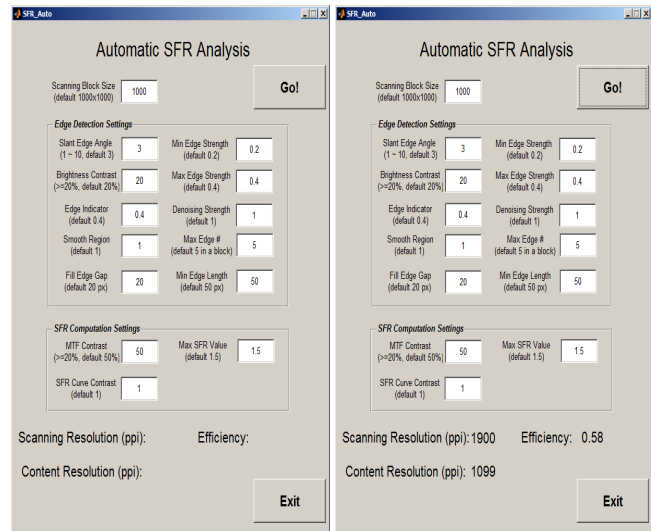


Figure 3. The user interface for autoSFR. Left: before running; Right: after running, the results are shown at the bottom.

## 4. Experiments

In our experiments, we tested our approach on a large set of 35mm photographic negatives (primarily nitrate-base) from the Farm Security Administration (FSA) Collection at the Library of Congress. The images were captured on a Stokes Imaging digital camera SII75M utilizing a Dalsa FTF5066C CCD array in 4-shot mode (approx. 33 MP). The FSA Collection contains documentary

photographs produced by U.S. Government photographers during the Great Depression and World War II (1936-1945).

The first experiment is to conduct the hypothesis test to compare the results obtained from the manually identified edges and those detected by the software. Our expert identified 100 edge regions from a selected set of ten images from the FSA collection. From the same set of ten source images, the autoSFR software automatically detected a total of 51 edge regions. With Eqs. (2), (3), (4), we compare the mean and variance of the sampling efficiency of these two sample sets using the two-sample  $t$ -test and  $F$ -test. For generality we use 5% significance level. The computed  $p$ -values are 0.087 and 0.7644 for the two-sample  $t$ -test and  $F$ -test respectively, which indicates a failure to reject the null hypothesis, i.e., the sampling efficiency from the two edge sets have statistically the same mean and variance. Therefore, the algorithm obtains similar results as the expert, which shows its robustness and accuracy.

In the second experiment, we test the denoising effects on the SFR and sampling efficiency computation. Figure 4 shows an artificial edge image, and the same image with Gaussian noise of different degree, e.g., variance  $\sigma^2 = 0.1$  and  $0.2$ . We apply Gaussian smoothing on the whole image except the narrow band surrounding the edge. Figure 5 shows the SFR curves corresponding to the images in Figure 4. It can be seen that the stronger noise introduces larger reduction on sampling efficiency. The sampling efficiency values corresponding to the minor and strong noise images are 52% and 26%, respectively. This observation is also consistent with the results presented in [18]. Figure 6 and 7 present the SFR curves after applying Gaussian filtering on the minor noise image (the middle image in Figure 4) with different parameter settings, i.e., minor and strong denoising (see Figure 6); narrow and wide band surrounding the edge (see Figure 7). In Figure 6, we can see that denoising improves the sampling efficiency values. However, it is difficult to draw the formal conclusion from this single example due to the very noisy SFR curves even after denoising. Meanwhile, the band size has almost no effects on the SFR and efficiency computation, as shown in Figure 7.

To further verify the denoising effects on the computation, we repeat the previous two-sample  $t$ -test and  $F$ -test to compare the sampling efficiency before and after the denoising on the same ten images in the first experiment. With narrow band (i.e., radius  $r = 1$  pixel for an edge point) preserved in smoothing, both minor ( $\sigma = 0.5$ ) and strong ( $\sigma = 2$ ) filtering produce statistically the same results as those without denoising. Only very strong denoising ( $\sigma = 20$ ) change the statistics. Meanwhile, with strong denoising, both narrow ( $r = 1$ ) and wide band ( $r = 5$ ) settings obtain the same results. Over this spatial region, we draw the tentative conclusion that both the denoising strength and the band size have insignificant effects on the SFR and sampling efficiency. It is likely that stronger de-noising has a greater effect on the precision of the SFR estimate than does the band width of the edge window. Further investigations to prove this are necessary though.

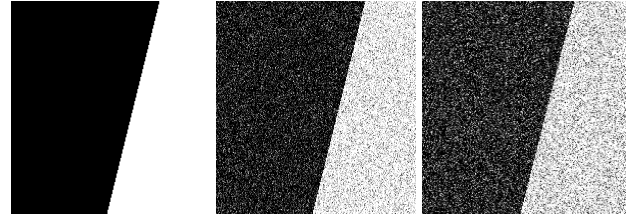


Figure 4. Synthetic edge image. Left: original image; Middle: small noise ( $\sigma^2 = 0.1$ ); Right: large noise ( $\sigma^2 = 0.2$ ).

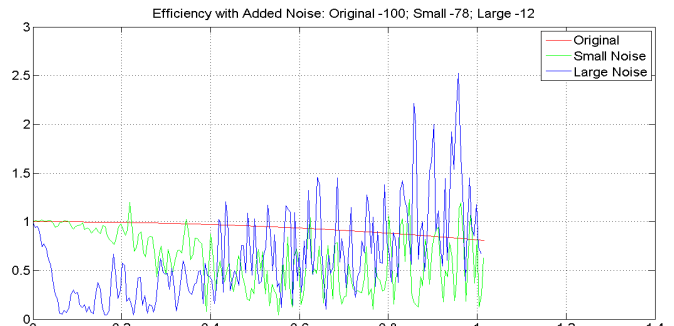


Figure 5. Sample efficiency values for Figure 4 images.

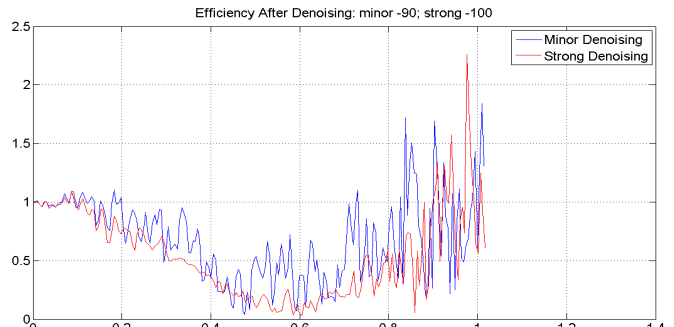


Figure 6. SFR curves after applying Gaussian smoothing on the middle image in Figure 4 with different standard deviation (minor: 0.5; strong: 2)

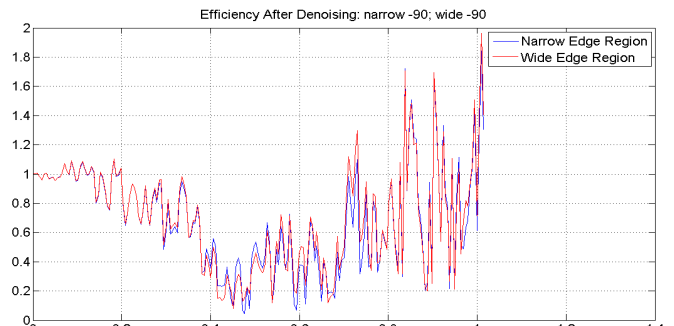


Figure 7. SFR curves after applying Gaussian smoothing on the middle image in Figure 4 with different sizes of band surrounding the edge (narrow: 1 pixel radius for an edge point; wide: 5 pixels radius for an edge point)

## 5. Conclusion

We extend our previous work of automated spatial resolution determination for digitization. The extension work includes: conducting hypothesis test to verify the robustness and accuracy of the algorithm, analyzing the denoising effects on the SFR and sampling efficiency computation, and constructing a user friendly interface for software distribution. Based on these explorations, we show that the algorithm is robust and can obtain comparable results with manual selection. Denoising generally introduces minor changes to the SFR and sampling efficiency computation but needs a more thorough investigation to draw strong conclusions. For future work, we will further investigate the above results on more comprehensive collections with larger sample sets.

## References

- [1] ISO 12233:2000, Photography – Electronic Still Picture Cameras – Resolution Measurements.
- [2] ISO 16067-1:2003, Photography – Spatial Resolution Measurements of Electronic Scanners for Photographic Images – Part 1: Scanners for Reflective Media.
- [3] ISO 16067-2:2004, Photography – Electronic Scanners for Photographic Images – Spatial Resolution Measurements – Part 2: Film Scanners.
- [4] ISO 14524:2009, Photography – Electronic Still Picture Cameras – Methods for Measuring Opto-Electronic Conversion Functions (OECFs).
- [5] ISO 13656:2000, Graphic Technology – Application of Reflection Densitometry and Colorimetry to Process Control or Evaluation of Prints and Proofs.
- [6] ISO 19084, Photography – Digital Cameras – Lateral Chromatic Displacement Measurement.
- [7] ISO 15739:2003, Photography – Electronic Still Picture Imaging – Noise Measurements.
- [8] ISO 21550:2004, Photography – Electronic Scanners for Photographic Images – Dynamic Range Measurements.
- [9] ISO 15529:2007, Optics and Optical Instruments – Optical Transfer Function – Principles of Measurement of Modulation Transfer Function (MTF) of Sampled Imaging Systems.
- [10] ISO 17850, Photography – Digital Cameras – Geometric Distortion Measurements.
- [11] E.M. Grainger, K.N. Cupery, “An Optical Merit Function (SQF) Which Correlates with Subjective Image Judgements,” *Photographic Science and Engineering*, 16, 3 (1972).
- [12] E. Samei, M.J. Flynn, D.A. Reimann, “A Method for Measuring the Presampled MTF of Digital Radiographic Systems Using an Edge Test Device,” *Medical Physics*, 25, 1 (1998).
- [13] H. Fujita, D. Tsai, T. Itoh, K. Doi, J. Morishita, K. Ueda, A. Ohtsuka, “A Simple Method for Determining the Modulation Transfer Function in Digital Radiography,” *IEEE Trans. On Medical Imaging*, 11, 1 (1992).
- [14] P.D Burns, Tone-Transfer (OECF) Characteristics and Spatial Frequency Response Measurements for Digital Cameras and Scanners, *Proc. SPIE*, pg. 123-128, 2005.
- [15] P.D Burns, D. Williams, Sampling Efficiency in Digital Camera Performance Standards, *Proc. SPIE*, pg. 937-940. (2008).
- [16] L. He, P. Michel, S. Puglia, D. Williams, Computer Assisted Image Analysis for Objective Determination of Scanning Resolution for Photographic Collections – An Automated Approach, *Proc. IS&T Archiving*, pg. 43-47. (2013).
- [17] S.G. Elkadiki, R.M. Rangayyan, Objective Characterization of Image Acutance, *Proc. SPIE*, pg. 210-218. (1994).
- [18] U. Artmann, D. Wueller, Differences of Digital Camera Resolution Metrology to Describe Noise Reduction Artifacts, *Proc. SPIE-IS&T Electronic Imaging*, pg. 75290L-1-12. (2010).
- [19] J. McElvain, S.P. Campbell, J. Miller, E.W. Jin, Texture-based Measurement of Spatial Frequency Response Using the Dead Leaves Target: Extensions, and Application to Real Camera Systems, *Proc. SPIE-IS&T Electronic Imaging*, pg. 75370D-1-11. (2010).
- [20] R. Ferzli, L.J. Karam, “A No-reference Objective Image Sharpness Metric Based on the Notion of Just Noticeable Blue (JNB),” *IEEE Trans. On Image Processing*, 18, 4 (2009).
- [21] N.D. Narvekar, L.J. Karam, A No-reference Perceptual Image Sharpness Metric Based on A Cumulative Probability of Blur Detection, *Proc. IEEE International Workshop on Quality of Multimedia Experience*, pg. 87-91. (2009).
- [22] D. Moore, G.E. McCabe, B. Craig, *Introduction to the Practice of Statistic* (W.H. Freeman, 7<sup>th</sup> Ed., 2010).

## Author Biography

*Lei He received his PhD in electrical engineering from University of Cincinnati (2003). Since then he has worked as a faculty member in the Department of Computer Science and Information Technology at Armstrong Atlantic State University in Savannah, GA. From 2009 to 2011, he visited the National Institutes of Health. Currently he is a digital imaging scientist at the Library of Congress. His work has focused on the image processing, computer vision and machine learning.*

*Phil Michel is a Digital Conversion Coordinator in the Library of Congress Prints & Photographs Division. He manages the Division's digitization program which includes over 1.3 million digitized items. Phil also participates in the Federal Agencies Digitization Guidelines Initiative and works actively on digital preservation and image lifecycle issues.*

*Steven Puglia worked as a Digital Conversion Services Manager at the Library of Congress. Previously he worked as a Preservation and Imaging Specialist at the US National Archives and Records Administration for over 22 years. He also coordinated the Still Imaging Working Group of the Federal Agencies Digitization Guidelines Initiative.*

*Don Williams worked as a research imaging scientist for Kodak for 25 years until he left to form his own company, Image Science Associates, in 2006. He has published extensively on both technical and policy matters as they relate to digital image fidelity and metrology. Don is also the editor for ISO 12233, 2nd edition, Spatial Resolution Measurements, Digital Still Cameras, and has acted as co-leader for equivalent performance standards on reflection and film scanners.*